



## Growth and Characterization of Irradiated Organoids from Mammary Glands

Benjamin C. Hacker<sup>1</sup>, Javier D. Gomez<sup>1</sup>, Carlos A. Silvera Batista<sup>1</sup>, Marjan Rafat<sup>1,2,3</sup>

<sup>1</sup>Department of Chemical and Biomolecular Engineering, Vanderbilt University

<sup>2</sup>Department of Biomedical Engineering, Vanderbilt University

<sup>3</sup>Department of Radiation Oncology, Vanderbilt University Medical Center

### Abstract

Organoids derived from the digested tissue are multicellular three-dimensional (3D) constructs that better recapitulate in vivo conditions than cell monolayers. Although they cannot completely model in vivo complexity, they retain some functionality of the original organ. In cancer models, organoids are commonly used to study tumor cell invasion. This protocol aims to develop and characterize organoids from the normal and irradiated mouse mammary gland tissue to evaluate the radiation response in normal tissues. These organoids can be applied to future in vitro cancer studies to evaluate tumor cell interactions with irradiated organoids. Mammary glands were resected, irradiated to 20 Gy and digested in a collagenase VIII solution. Epithelial organoids were separated via centrifugal differentiation, and 3D organoids were developed in 96-well low-adhesion microplates. Organoids expressed the characteristic epithelial marker cytokeratin 14. Macrophage interaction with the organoids was observed in co-culture experiments. This model may be useful for studying tumor-stromal interactions, infiltration of immune cells, and macrophage polarization within an irradiated microenvironment.

### Keywords

Bioengineering; Issue 147; 3D organoid culture; mammary gland; normal tissue radiation response; cell-cell interactions; breast cancer; cancer immunology

### Introduction

Approximately 60% of the triple negative breast cancer (TNBC) patients choose breast-conserving therapy (BCT) as a form of treatment<sup>1</sup>. In this treatment modality, the tumor containing part of the breast tissue is removed, and the surrounding normal tissue is exposed to ionizing radiation to kill any residual tumor cells. Treatment reduces recurrence in much of the breast cancer population; however, approximately 13.5% of treated patients with

---

Correspondence to: Marjan Rafat at [marjan.rafat@vanderbilt.edu](mailto:marjan.rafat@vanderbilt.edu).

Disclosures

The authors have nothing to disclose.

Video Link

The video component of this article can be found at <https://www.jove.com/video/59293/>

TNBC experience locoregional recurrences<sup>2</sup>. Therefore, studying how radiation may recruit circulating tumor cells (CTCs) will lead to important insights into local recurrence<sup>3,4</sup>.

Previous work has shown that radiation of the normal tissue increases recruitment of various cell types<sup>5</sup>. In pre-clinical models of TNBC, irradiation of normal tissue increased macrophage and subsequently tumor cell recruitment to normal tissues<sup>5</sup>. Immune status influenced tumor cell recruitment to irradiated sites, with tumor cell migration observed in immunocompromised subjects. Recapitulating these interactions using organoids derived from mammary glands will allow the observation of cell migration and cell-stromal interactions in real time with microscopy and live cell imaging to determine the role of radiation damage in altering tumor cell behavior.

Mouse mammary organoids have helped elucidate key steps in the development of the mammary gland. A mammary organoid is a multicellular, three dimensional construct of isolated mammary epithelium that is larger than 50  $\mu\text{m}$ <sup>6,7,8,9,10</sup>. Using primary epithelial organoids, Simian et al. evaluated necessary factors for branching in the mammary gland<sup>7</sup>. Shamir et al. discovered that dissemination can occur without an epithelial to mesenchymal transition, providing insight into the metastatic cascade<sup>8</sup>. Methods for generating and characterizing organoids from mammary gland tissue are well established<sup>6,11,12,13</sup>. However, to our knowledge, methods for growing irradiated organoids from mammary glands have not been reported. A protocol for growing and characterizing irradiated organoids would be a critical step in recapitulating radiation-induced immune and tumor cell recruitment.

In this paper, we report a method for growing and characterizing irradiated mammary epithelial organoids in low adhesion microplates coated with a hydrophilic polymer that supports the formation of spheroids. These organoids were co-cultured with macrophages to examine immune cell infiltration kinetics. This work can be extended to include co-culturing organoids with adipose cells to recapitulate mammary characteristics, breast cancer cells to visualize tumor cell recruitment, and CD8+ T cells to study tumor-immune cell interactions. Previously established protocols may be used to evaluate irradiated organoids. Earlier models co-culturing mammary organoids and immune cells have shed light on mechanisms of metastasis and dissemination. DeNardo et al. found that CD4+ T cell regulation of tumor associated macrophages enhanced a metastatic phenotype of mammary adenocarcinomas<sup>14</sup>. Co-culture models have also been used to elucidate mechanisms of biological development. Plaks et al. clarified the role of CD4+ T cells as down-regulators of mammary organogenesis<sup>15</sup>. However, our group is the first to establish a procedure of visualizing how normal tissue irradiation influences immune cell behavior. Because normal tissue irradiation has been shown to enhance tumor cell recruitment<sup>5</sup>, this protocol can be further developed to analyze how tumor cell behavior is altered by irradiation of normal tissue and cells, leading to a greater understanding of cancer recurrence.

## Protocol

Animal studies were performed in accordance with institutional guidelines and protocols approved by the Vanderbilt University Institutional Animal Care and Use Committee.

## 1. Preparation of mice and cell acquisition (adapted from Nguyen-Ngoc et al.<sup>11</sup>)

1. Sacrifice athymic Nu/Nu mice (8–10 weeks old) using CO<sub>2</sub> asphyxiation followed by cervical dislocation. Clean the skin using 70% ethanol.
2. Resect abdominal and inguinal mammary glands from mice using pre-sterilized scissors and forceps. Remove lymph nodes before resection. Rinse in sterile 1× phosphate buffered saline (PBS) (Figure 1A).
3. Place it in 15 mL tubes with 10 mL of Dulbecco's Modified Eagle Media/ Nutrient Mixture F12 (DMEM/F12) for transport. Samples can be kept overnight at 4 °C or processed immediately. Keep on ice.
4. Irradiate samples at 20 Gy using a cesium source (Figure 1B).
5. 45 min after irradiation, place mammary glands in a 35 mm sterile cell plate and mince with scalpels (Figure 1C,D). Mince with approximately 40 strokes until the tissue relaxes and pieces are obtained that are no larger than approximately 1 mm<sup>2</sup> in area.
6. Transfer to the collagenase solution in a 50 mL centrifuge tube. Collagenase solution consists of 2 mg/mL collagenase (see **Table of Materials**), 2 mg/mL trypsin, 5% v/v fetal bovine serum (FBS), 5 µg/mL insulin, and 50 µg/mL gentamicin in DMEM/F12 media. Use 10 mL collagenase solution per mouse.
7. Place in a water bath at 37 °C, vortexing every 10 min for 30–60 min. Digestion is complete when the collagenase solution is cloudy (Figure 1E,F).
8. Spin down the digested solution at 450 × *g* for 10 min at room temperature (RT). Three layers will be observed. The supernatant is composed of fat, the middle layer is an aqueous solution, and the bottom is a pellet. The pellet will appear red as it is a mixture of epithelial cells, individual stromal cells, and red blood cells (Figure 1G).
9. Precoat all pipettes, pipette tips, and centrifuge tubes with bovine serum albumin (BSA) solution prior to contact. BSA solution consists of 2.5 w/v % BSA in Dulbecco's Phosphate Buffered Saline (DPBS). For pre-coating, simply add then remove BSA solution to the inside of the pipette tip and tubes. BSA solution can be reused, although it should be sterile filtered before each experiment.
10. For additional recovery, transfer the supernatant to a fresh BSA coated 15 mL tube. Pipette up and down vigorously to disperse fat layer. Centrifuge at 450 × *g* for 10 min at RT. Aspirate the supernatant, leaving a small amount of media in the tube to avoid aspirating the cell pellet.
11. Aspirate the aqueous layer from the tube with the original pellet.
12. Add 10 mL of DMEM/F12 to the tube with the original pellet and transfer to the second tube. Pipette vigorously to combine and resuspend the two pellets.
13. Centrifuge at 450 × *g* for 10 min at RT. Aspirate the supernatant and add 4 mL of DMEM/F12 to the tube.

14. Add 40  $\mu\text{L}$  of deoxyribonuclease (DNase) to the suspension and gently shake by hand for 2–5 min at RT. DNase solution consists of 4 U/mL DNase in DMEM/F12.
15. Add 6 mL of DMEM/F12 and pipette thoroughly. Centrifuge the tube at  $450 \times g$  for 10 min at RT.
16. Aspirate supernatant to the 0.5 mL mark. Resuspend in 10 mL of DMEM/F12 and pipette thoroughly.
17. Pulse to  $450 \times g$  and stop 4 s after reaching that speed.
18. Repeat steps 1.16–1.17 three more times to purify organoids via centrifugal differentiation. The pellet should now be an off-white color consisting of only epithelial organoids (Figure 1H).

NOTE: Organoids can also be filtered using sterile mesh 40  $\mu\text{m}$  filters. After step 1.16, pipette media containing organoids through a filter into a centrifuge tube, and then rinse with 5 to 10 mL of DMEM/F12 media. Flip the filter over a new 50 mL centrifuge tube. Pass 10 mL of DMEM/F12 media through, going the opposite way to rinse off any retentate. The retentate should consist of organoids, and the filtrate should consist mainly of stromal cells, which can be discarded or kept if desired.

## 2. Determining density and plating organoids

1. Resuspend pellet in 10 mL of DMEM/F12. Pipette thoroughly to create a homogenous solution.
2. Transfer 50  $\mu\text{L}$  to a 30 mm Petri dish, and view under a phase contrast microscope at  $20\times$ . Count the number of organoids with a tally counter.

NOTE: Here pipette tips have been consistently used with a minimal diameter of 457  $\mu\text{m}$ , which is 5–10 times the diameter of the organoids that are seeded. For transferring volumes of 2 mL or larger (e.g., steps 1.16 and 2.1), use serological pipettes with tip diameters excess of 1,500  $\mu\text{m}$ .

3. Calculate the organoid density using the following equation:

$$\frac{\# \text{ organoids in } 50\mu\text{L}}{50\mu\text{L}} = \frac{\# \text{ organoids in tube}}{\text{volume of tube}} [=] \frac{\text{organoids}}{\mu\text{L}}.$$

The desired density is 1,000 organoids/mL to simplify further dilution. If the density is too low, centrifuge at  $450 \times g$  for 5 min and aspirate media. Add media necessary to reach 1,000 organoids/mL, and pipette thoroughly to create a homogenous mixture.

1. To grow organoids in a protein matrix, seed organoids at a concentration of 1 organoid/L in collagen type 1 diluted to 87% or in basement membrane extracted from Engelbreth-Holm-Swarm mouse sarcoma. While working with samples, keep on ice.

2. To freeze organoids, transfer the desired volume to a separate centrifuge tube. Spin down at  $450 \times g$  for 5 min. Aspirate media, and then add the same volume of 90% FBS/10% DMSO. Resuspend the organoids, and then aliquot into cryotubes. Transfer to  $-80\text{ }^{\circ}\text{C}$ , and then to liquid nitrogen within one week.
3. To thaw, warm in a  $37\text{ }^{\circ}\text{C}$  water bath for one min. Centrifuge at  $450 \times g$  for 5 min, and then aspirate freezing media. Rinse with sterile DPBS, and then centrifuge again. Aspirate DPBS and add organoid media.
4. Pipette 50 03BCL (50 organoids) into each well of the low adhesion plate (Figure 1I).
5. Add 150  $\mu\text{L}$  of organoid media to bring the total working volume to 200  $\mu\text{L}$ . Organoid media consists of 1% penicillin-streptomycin and 1% insulin-transferrin-selenium (ITS) in DMEM/F12 media.
6. Every 2 days replace media carefully.

NOTE: Low adhesion plates are not tissue culture treated; therefore, the cells can be easily detached. Aspirate media slowly by tilting the plate and inserting the pipette tip at the edge of each well. Leave a small amount of media in the bottom of the well. Add new media slowly to avoid applying unnecessary shear forces to organoids.

### 3. Co-culturing with macrophages

1. Maintain GFP or dTomato-labelled RAW 264.7 macrophages in DMEM media supplemented with 10% FBS and 1% penicillin-streptomycin. Seed  $1 \times 10^4$ ,  $5 \times 10^4$ , or  $1 \times 10^5$  cells/mL into organoid media.
2. Use live cell phase contrast and fluorescent imaging to monitor macrophage infiltration over time.

### 4. Immunofluorescence staining of organoids

NOTE: Organoids can be stained in low adhesion wells or can be transferred to chamber slides. To transfer, gently pipette up and down until organoids have detached from plates. Transfer to chamber slides and incubate for 4–8 h to allow organoids to adhere to the plate surface.

1. Remove organoid medium from the wells by carefully aspirating. Fix samples with 10% neutral buffered formalin for 15 min at RT.
2. Wash  $3 \times 5$  min in 1x PBS. If desired, fixed samples can be stored at  $4\text{ }^{\circ}\text{C}$  for one week for further staining.
3. Permeabilize with 0.1% 4-(1,1,3,3-Tetramethylbutyl) phenyl-polyethylene glycol for 5 min.

NOTE: To stain for F-actin, incubate samples with phalloidin diluted 1:1,000 and 1.67 nM bisbenzimidazole nuclear dye in 1% PBS/BSA for 1 h at RT. Then, proceed to step 4.8.

4. Permeabilize with 0.5% PBS. Samples can be stored at 4°C. Images can be taken as brightfield or immunofluorescent images. Mechanisms that contribute to CTC block with 5% normal goat serum in 0.1% PBS/Polyethylene glycol sorbitan monolaurate (PBST) for 1 h at RT. Wash 3 × 5 min with PBS.
5. Incubate with Anti-Cytokeratin 14 diluted 1:1,000, E-Cadherin diluted 1:200, or Tight Junction Protein One diluted 1:100 in 1% NGS in PBST for 1 h at RT. Wash 3 × 5 min in PBST.
6. Incubate with Goat Anti-Rabbit secondary diluted 1:200 with 1% NGS/PBST for 1 h at RT. Cover with foil to avoid light exposure.
7. Wash 3 × 5 min in PBS. Use the nuclear dye (see **Table of Materials**) to stain nuclei.
8. Wash 3 × 5 min in PBS. If using chamber slide, mount with a coverslip. Store wrapped in foil at 4 °C for up to 2 weeks.

## Representative Results

Irradiated epithelial mammary organoids were successfully obtained from mouse mammary glands, processed, and cultured on low-adhesion plates (Figure 1). Organoid yield was tested by seeding in different growth environments (Figure 2A–G). Seeding cells directly onto tissue culture treated 10 cm cell plates yielded an overgrowth of fibroblast cells. Fibroblasts were identified under phase contrast microscopy in or near the same plane of focus as organoids, and they quickly grew out from plated organoids within a few days. An outgrowth of fibroblasts was also observed when organoids were seeded in basement membrane and collagen protein matrices (Figure 2E,F).

A variety of conditions were tested in optimizing irradiated organoid growth (Figure 2H). Collagenase types I and VIII from *Clostridium histolyticum* were used as the enzyme in the organoid digestion step<sup>12,16,17</sup>. Organoid yields were significantly higher after digestion with collagenase VIII. This may be due to the purification processes used in producing the enzyme: collagenase type I is partially purified and may cause unnecessary damage to membrane proteins and receptors, leading to poor organoid formation, cell lysis, or over-digestion<sup>16,17,18</sup>. No significant differences in yield between irradiated and control organoids were observed.

Irradiated organoids could be cultured in low adhesion plates (Figure 3A–C) or within basement membrane (Figure 3D–G), but the most rapid growth occurred in low adhesion plates (Figure 3H). Organoids recapitulated mammary gland characteristics. White arrowheads indicate constructs morphologically similar to ducts and lobes<sup>19,20,21</sup> (Figure 3C), which are critical for the production and transport of milk in the mammary gland<sup>21</sup>. However, further characterization is required to confirm this observation. Growth trends indicated that non-irradiated organoids grew faster than irradiated organoids (Figure 3H),

most likely due to cell growth arrest resulting from mechanisms of DNA damage repair; however, the trend was not statistically significant<sup>22</sup>. Occasional clumping of low adhesion organoids was observed, and organoids could be cultured up to two weeks before dissociating.

Organoids expressed epithelial characteristics, which were evaluated through immunofluorescence staining of Cytokeratin 14 (K14), E-Cadherin (E-cad), and Tight Junction Protein 1 (ZO-1)<sup>23,24,25</sup> (Figure 4). Irradiated organoids expressed epithelial markers. K14, a marker of myoepithelium<sup>23</sup>, was expressed strongly on the surface of irradiated organoids (Figure 4A). Additionally, E-cad and ZO-1 were expressed within cellular junctions of organoids (Figure 4B, C). These proteins are essential for proper cell adhesion<sup>24</sup>. After irradiation, organoids continued to retain their epithelial characteristics.

Fluorescent staining of organoids could be visualized within low adhesion plates using fluorescence microscopy (Figure 5A–D); however, the clearest visualization was obtained via confocal microscopy (Figure 5E–F). Corrected total fluorescence intensity was calculated by subtracting the background and normalizing by organoid area (Figure 5G). Growing organoids in the 96-well low adhesion plates also simplified co-culture experiments. When seeded at concentrations typical in the mammary gland, macrophages co-localized with control and irradiated organoids (Figure 6)<sup>24,26</sup>.

## Discussion

In this protocol, we have developed a method for reproducible growth and characterization of irradiated mammary organoids (Figure 1). An irradiation dose of 20 Gy was applied to mirror previous *in vivo* models of tumor cell recruitment<sup>5</sup>. Irradiation of mammary glands *ex vivo* prior to organoid formation allowed for isolation of radiation damage effects without a corresponding infiltration of immune cells. The development of an *in vitro* irradiated normal tissue model enables real time viewing of cellular interactions that may contribute to radiation induced CTC recruitment<sup>11,12</sup>.

Closely following steps 1.5–1.18 was critical for maximizing organoid yield. We added thawed aliquots of concentrated collagenase to the digestive solution. Due to the highly viscous nature of the concentrated collagenase aliquot, there can be some variations in amount and therefore in enzymatic activity, so organoid digestion must be closely monitored to avoid over-digestion. It is also important to digest organoids in a 50 mL tube as this allows for an even surface area for digestion. Other studies have used filtration for purifying organoids<sup>19,23</sup>; however, we obtained a much higher yield purifying with centrifugal differentiation (Figure 2H). Pre-coating pipettes, pipette tips, and centrifuge tubes with the BSA solution is essential for maximizing yield. Organoids noticeably adhere to uncoated plastic when solution application is neglected.

Great care must be taken to avoid aspirating organoids. This is a risk that occurs when purifying, changing media, and staining for fluorescent markers. Using low adhesion plates for growth allows for easy transfer of organoids and removes the need for organoids to be sectioned in OCT for further staining, a procedure required for basement membrane



embedded organoids<sup>11</sup>. In addition to benefits from superior growth, seeding irradiated organoids in low adhesion plates required fewer steps and was less technically challenging than culturing organoids in basement membrane or collagen. However, when staining for markers, it may be helpful to view organoids under a microscope to ensure that accidental aspiration does not occur.

Moreover, there are many considerations that must be accounted for when imaging organoids. Within basement membrane embedded organoids, occasional fibroblast growth may be observed (Figure 2C,D). Fibroblast outgrowth in 3D cultured organoids may be caused by organoids making contact with the tissue culture treated surface as adhesion leads to upregulated fibroblast growth factor production in adherent cells<sup>27</sup>. Interestingly, the morphology of these fibroblasts is strikingly similar to pre-adipocytes as both cell types exhibit spindly, elongated shapes<sup>28</sup>. In further investigation, exposure to insulin, dexamethasone, and 3-isobutyl-1-methylxanthine (IBMX) may yield cells with an adipogenic lineage, spurring a shift towards a more spherical cellular shape associated with adipocytes<sup>28,29</sup>. We obtained clear images using phase contrast microscopy of free-growing low adhesion (Figure 3A–C) and basement membrane embedded (Figure 3D–G) organoids. Tracking individual organoid growth in low adhesion plates, however, was difficult due to minimal focal adhesions between the cells and well surface, resulting in organoid movement and occasional aspiration.

Once stained for surface markers, confocal microscopy rendered clearer marker localization (Figure 5E,F) than widefield microscopy (Figure 5A–D). From fluorescence quantification, trends in phalloidin expression suggest that irradiated organoids expressed increased F-actin relative to the control (Figure 5G). Actin cytoskeleton reorganization has been observed in dermal microvascular endothelial cells irradiated at similar dosages<sup>30</sup>.

For extended imaging sequences, like time lapse co-culture with immune cells (Figure 6), a live cell imaging chamber with humidity and CO<sub>2</sub> control is required<sup>31</sup>. Live cell images taken every 30 minutes revealed that macrophages co-localized with organoids after 24 hours (Figure 6A,B), preferentially migrating toward irradiated organoids (Figure 6C). Macrophage infiltration into irradiated normal tissue has been observed in vivo, is attributed to chemokine and cytokine gradients, and typically precedes CTC recruitment<sup>5</sup>. Future studies will evaluate classically and alternatively activated macrophage interactions with organoids as polarized macrophage dynamics may play an important role in determining response to radiation<sup>32,33</sup>. Additional analyses will evaluate the consequence of serum starvation and the growth effects of culturing organoids in complete media since these variables may have significant effects on organoid-immune cell interactions. This system can further be adapted for co-culture with other cell types, including CD8+ T cells, stromal cells, adipocytes, and breast cancer cells. Real time observation with techniques like live cell imaging will facilitate the elucidation of potential mechanisms that contribute to CTC recruitment to irradiated normal tissue, which may have significant implications for patients suffering from recurrent TNBC.



## Acknowledgments

We thank Dr. Laura L. Bronsart for providing GFP and dTomato-labeled RAW 264.7 macrophages. This research was financially supported by NIH grant #R00CA201304.

## References

1. Lautner M et al. Disparities in the Use of Breast-Conserving Therapy Among Patients With Early-Stage Breast Cancer. *Journal of the American Medical Association Surgery*. 150 (8), 778–786 (2015). [PubMed: 26083835]
2. Lowery A, Kell M, Glynn R, Kerin M, Sweeney K Locoregional recurrence after breast cancer surgery: a systematic review by receptor phenotype. *Breast Cancer Research and Treatment*. 133, 831–841 (2012). [PubMed: 22147079]
3. Kim MY et al. Tumor Self-Seeding by Circulating Cancer Cells. *Cell*. 139 (7), 1315–1326 (2009). [PubMed: 20064377]
4. Vilalta M, Rafat M, Giaccia AJ, Graves EE Recruitment of Circulating Breast Cancer Cells Is Stimulated by Radiotherapy. *Cell Reports*. 8 (2), 402–409 (2014). [PubMed: 25017065]
5. Rafat M et al. Macrophages Promote Circulating Tumor Cell-Mediated Local Recurrence following Radiotherapy in Immunosuppressed Patients. *Cancer Research*. 78 (15), 4241–4252 (2018). [PubMed: 29880480]
6. Shamir ER, Ewald AJ Three-dimensional organotypic culture: Experimental models of mammalian biology and disease. *Nature Reviews Molecular Cell Biology*. 15 (10), 647–64 (2014). [PubMed: 25237826]
7. Simian M, Hirai Y, Navre M, Werb Z, Lochter A, Bissell MJ The interplay of matrix metalloproteinases, morphogens and growth factors is necessary for branching of mammary epithelial cells. *Development (Cambridge, England)*. 128, 3117–3131 (2001).
8. Shamir ER et al. Twist1-induced dissemination preserves epithelial identity and requires E-cadherin. *Journal of Cell Biology*. 204 (5), 839–856 (2014). [PubMed: 24590176]
9. Ewald AJ, Brenot A, Duong M, Chan BS, Werb Z Collective Epithelial Migration and Cell Rearrangements Drive Mammary Branching Morphogenesis. *Developmental Cell*. 14, 570–581 (2008). [PubMed: 18410732]
10. Nguyen-Ngoc K-V et al. ECM microenvironment regulates collective migration and local dissemination in normal and malignant mammary epithelium. *Proceedings of the National Academy of Sciences*. 89 (19), E2595–E2604 (2012).
11. Nguyen-Ngoc K-V, Shamir ER, Huebner RJ, Beck JN, Cheung KJ, Ewald AJ 3D Culture Assays of Murine Mammary Branching Morphogenesis and Epithelial Invasion. *Tissue Morphogenesis: Methods and Protocols*. 1189, 135–162 (2015).
12. Ewald AJ Isolation of mouse mammary organoids for long-term time-lapse imaging. *Cold Spring Harbor Protocols*. 8 (2), 130–133 (2013).
13. Drost J, Clevers H Organoids in cancer research. *Nature Reviews Cancer*. (2018).
14. DeNardo DG et al. CD4+T Cells Regulate Pulmonary Metastasis of Mammary Carcinomas by Enhancing Protumor Properties of Macrophages. *Cancer Cell*. 16 (2), 91–02 (2009). [PubMed: 19647220]
15. Plaks V et al. Adaptive Immune Regulation of Mammary Postnatal Organogenesis. *Developmental Cell*. 34 (5), 493–504 (2015). [PubMed: 26321127]
16. Mandl I, McLennan JD, Howes EL Isolation and Characterization of Proteinase and Collagenase From *Cl. histolyticum*. *The Journal of Clinical Investigation*. 32, 1323–1329 (1953). [PubMed: 13109000]
17. Mandl I, Zaffuto SF Serological Evidence for a Specific *Clostridium histolyticum* Gelatinase. *The Journal of General Microbiology*. 18, 13–15 (1958). [PubMed: 13525623]
18. Bond MD, Van Wart HE Characterization of the Individual Collagenases from *Clostridium histolyticum*. *Biochemistry*. 23 (13), 3085–3091 (1984). [PubMed: 6087888]
19. Zhang L et al. Establishing estrogen-responsive mouse mammary organoids from single Lgr5+ cells. *Cellular Signalling*. 29, 41–51 (2016). [PubMed: 27511963]

20. Sokol ES, Miller DH, Breggia A, Spencer KC, Arendt LM, Gupta PB Growth of human breast tissues from patient cells in 3D hydrogel scaffolds. *Breast Cancer Research*. 18 (1), 1–13 (2016). [PubMed: 26728744]
21. Richert MM et al. An atlas of mouse mammary gland development. *Journal of Mammary Gland Biology and Neoplasia*. 5 (2), 227–41 (2000). [PubMed: 11149575]
22. Maier P, Hartmann L, Wenz F, Herskind C Cellular pathways in response to ionizing radiation and their targetability for tumor radiosensitization. *International Journal of Molecular Sciences*. 17 (1) (2016).
23. LaBarge MA, Garbe JC, Stampfer MR Processing of Human Reduction Mammoplasty and Mastectomy Tissues for Cell Culture. *Journal of Visualized Experiments*. (71), 1–7 (2013).
24. Campbell JJ, Botos LA, Sargeant TJ, Davidenko N, Cameron RE, Watson CJA 3-D in vitro co-culture model of mammary gland involution. *Integrative Biology (United Kingdom)*. 6, 618–626 (2014).
25. Chanson L et al. Self-organization is a dynamic and lineage-intrinsic property of mammary epithelial cells. *Proceedings of the National Academy of Sciences*. 14 (7), 2293–2306 (2011).
26. Chua ACL, Hodson LJ, Moldenhauer LM, Robertson SA, Ingman W V Dual roles for macrophages in ovarian cycle-associated development and remodelling of the mammary gland epithelium. *Development (Cambridge, England)*. 137, 4229–4238 (2010).
27. Ingber D, Folkman J Mechanochemical switching between growth and differentiation during fibroblast growth factor-stimulated angiogenesis in vitro: role of extracellular matrix. *The Journal of Cell Biology*. 109 (7), at <<http://jcb.rupress.org/content/109/1/317.abstract>>(1989).
28. Gregoire FM, Smas CM, Sul HS Understanding Adipocyte Differentiation. *Physiological Reviews*. 78 (3), 783–809 (1998). [PubMed: 9674695]
29. Scott MA, Nguyen VT, Levi B, James AW Current Methods of Adipogenic Differentiation of Mesenchymal Stem Cells. *Stem Cells and Development*. 20 (10), 1793–1804 (2011). [PubMed: 21526925]
30. Gabry D, Greco O, Patel G, Prise KM, Tozer GM, Kanthou C Radiation Effects on the Cytoskeleton of Endothelial Cells and Endothelial Monolayer Permeability. *International Journal of Radiation Oncology, Biology, Physics*. 69 (5), 1553–1562 (2007).
31. Ewald AJ Practical considerations for long-term time-lapse imaging of epithelial morphogenesis in three-dimensional organotypic cultures. *Cold Spring Harbor Protocols*. 8, 100–117 (2013).
32. Zhang M et al. A high M1/M2 ratio of tumor-associated macrophages is associated with extended survival in ovarian cancer patients. *Journal of Ovarian Research*. 7 (1), 1–16 (2014). [PubMed: 24401654]
33. Ma J, Liu L, Che G, Yu N, Dai F, You Z The M1 form of tumor-associated macrophages in non-small cell lung cancer is positively associated with survival time. *BioMed Central Cancer*. 10, 112 (2010). [PubMed: 20338029]

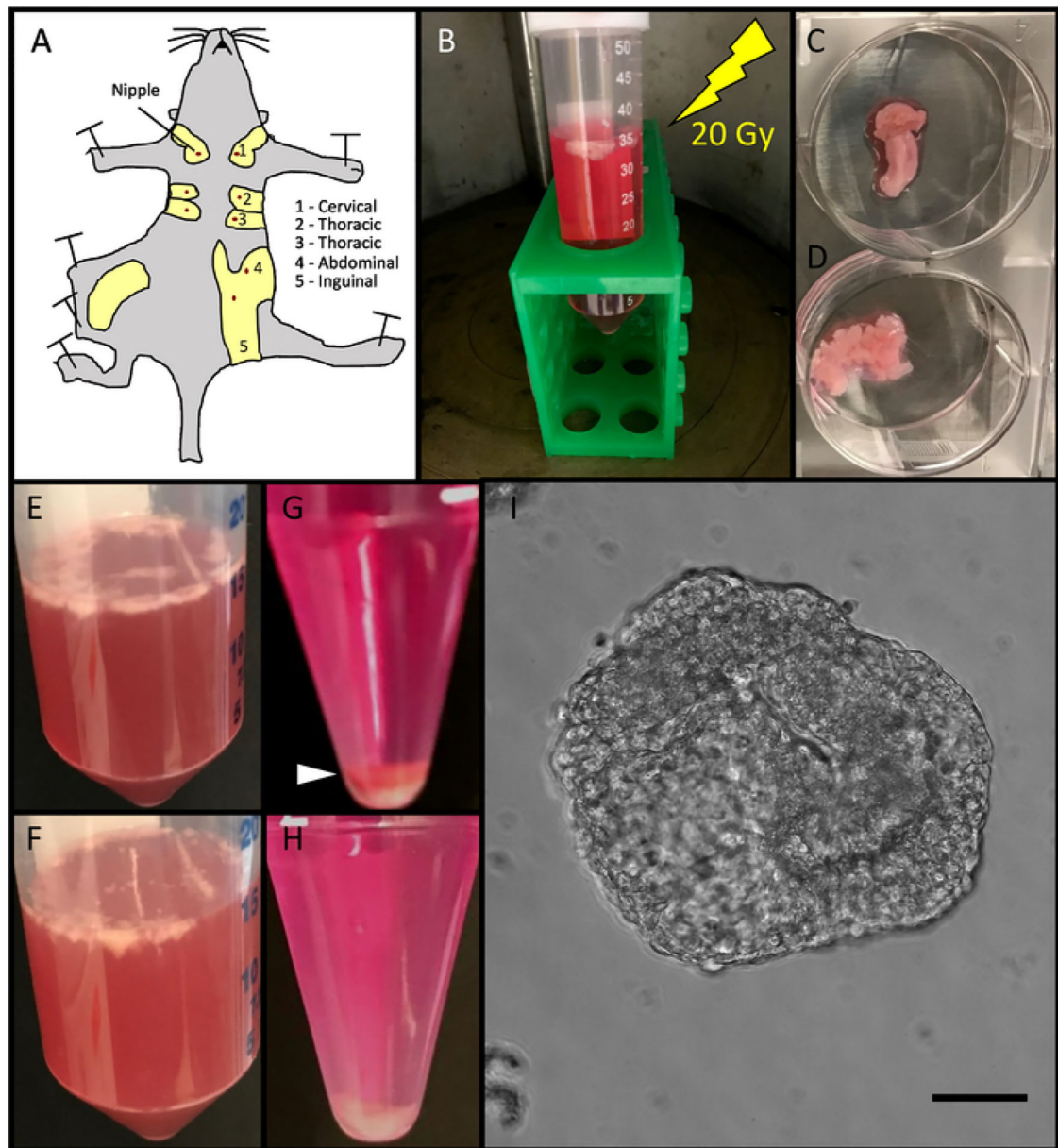


**Figure 1. Method Workflow.**

(A) Mammary glands were resected from mice. The abdominal and inguinal mammary glands were used. (B) Mammary glands were irradiated in 50 mL centrifuge tubes containing DMEM/F12 media. (C) Mammary glands were transferred to sterile six-well plates and cut with surgical scalpels until minced (D). (E) Mammary glands were transferred into 50 mL centrifuge tubes containing 5 mL of sterile DMEM/F12 media per gland and digested in a collagenase VIII solution (F). (G) After being transferred to a 15 mL tube, centrifugal differentiation was utilized to remove stromal cells, single cells, and red blood cells, observed in a red pellet (white arrow-head) until only white epithelial organoids were obtained (H). (I). 50 organoids were plated in 200  $\mu$ L of media in 96-well low adhesion

plates and imaged using phase contrast microscopy Scale bar represents 50  $\mu\text{m}$ . Please click here to view a larger version of this figure.

Author Manuscript

Author Manuscript

Author Manuscript

Author Manuscript

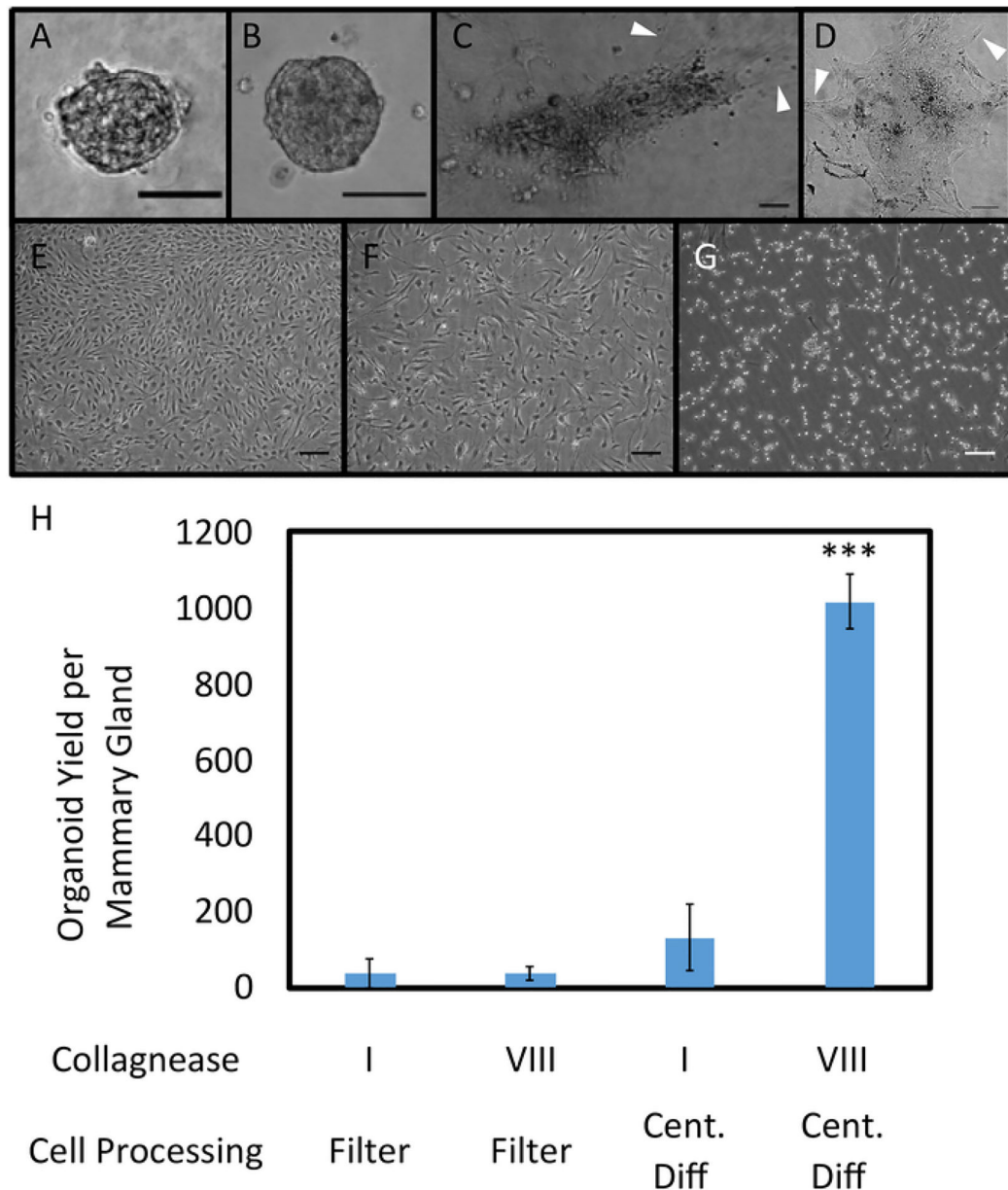


**Figure 2. Organoid Plating in 3D Protein Matrices and on Tissue Culture Treated Plastic.** Organoids seeded in collagen (A) and basement membrane (B), imaged after 84 hours of growth. Outgrowth of fibroblasts occurred in matrix plated organoids (C, D). Phase contrast images of organoids sorted through filtration were obtained 192 hours after seeding. No major differences between the filtrate (E) and retentate (F) were observed, with both resulting in confluent fibroblast growth. Cells in E and F were seeded on tissue culture treated plastic. After trypsinizing for 5 min at RT, fibroblasts were removed via aspiration; however, remaining epithelial cells formed a monolayer culture instead of three-dimensional organoids (G). Scale bars for A-G represent 100  $\mu$ m. (H) Different collagenase types (I (CI) and VIII (CVIII)) and cell processing methods (filtration and centrifugal differentiation (Cent Diff)) were tested, and organoid yield per mammary gland was quantified (n = 2

glands for CI, Filter; 2 glands for CVIII, Filter; 4 glands for CI, Cent Diff, and 12 glands for CVIII, Cent Diff). Statistical significance was determined using a two-tailed, unpaired t-test, \*\*\* $p < 0.0001$ . Error bars represent standard error. Please click [here](#) to view a larger version of this figure.

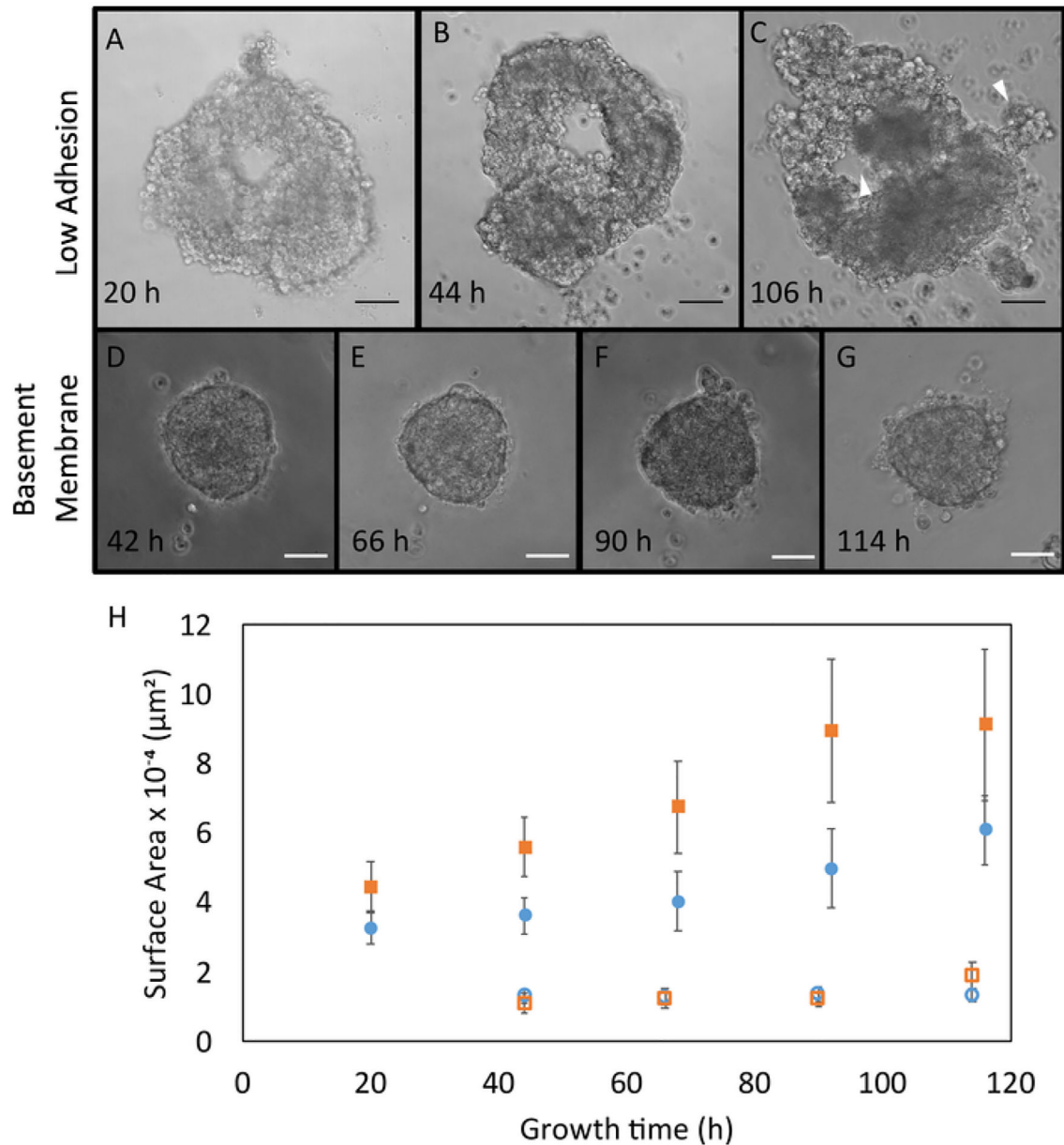
Author Manuscript

Author Manuscript

Author Manuscript

Author Manuscript







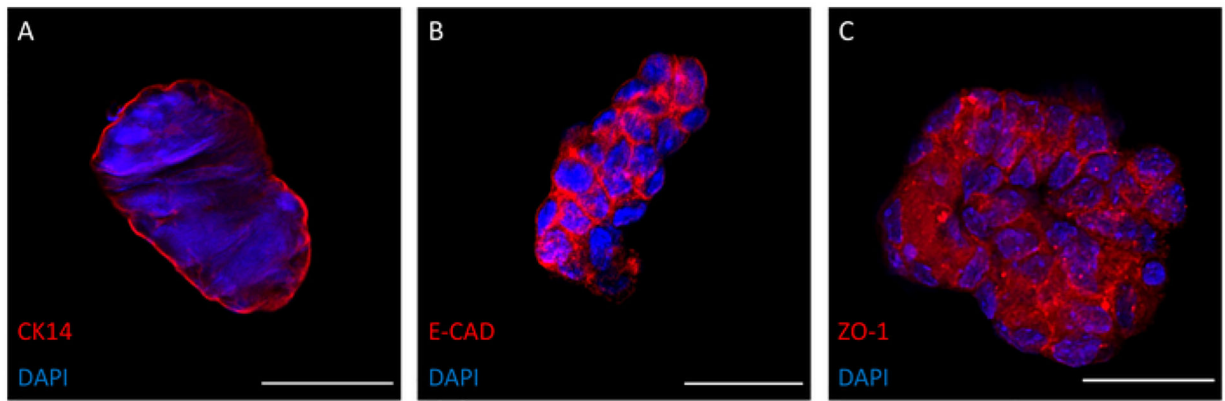


**Figure 4. Epithelial Marker Expression on Irradiated Organoids.**

Cytokeratin 14 (K14, green), a marker for the basal layer of squamous and non-squamous epithelia, was expressed on irradiated organoids (A). E-cadherin (E-Cad), a protein essential for adhesion, was expressed within the junctions between cells in irradiated organoids (B). Tight junction protein one (ZO-1) was also expressed within cell junctions of irradiated organoids (C). Images were obtained in chamber slides via confocal microscopy. A nucleic acid stain was used to visualize nuclei (blue). All organoids were fixed and imaged after one week of growth. Scale bars are 50 $\mu$ m. Please click here to view a larger version of this figure.

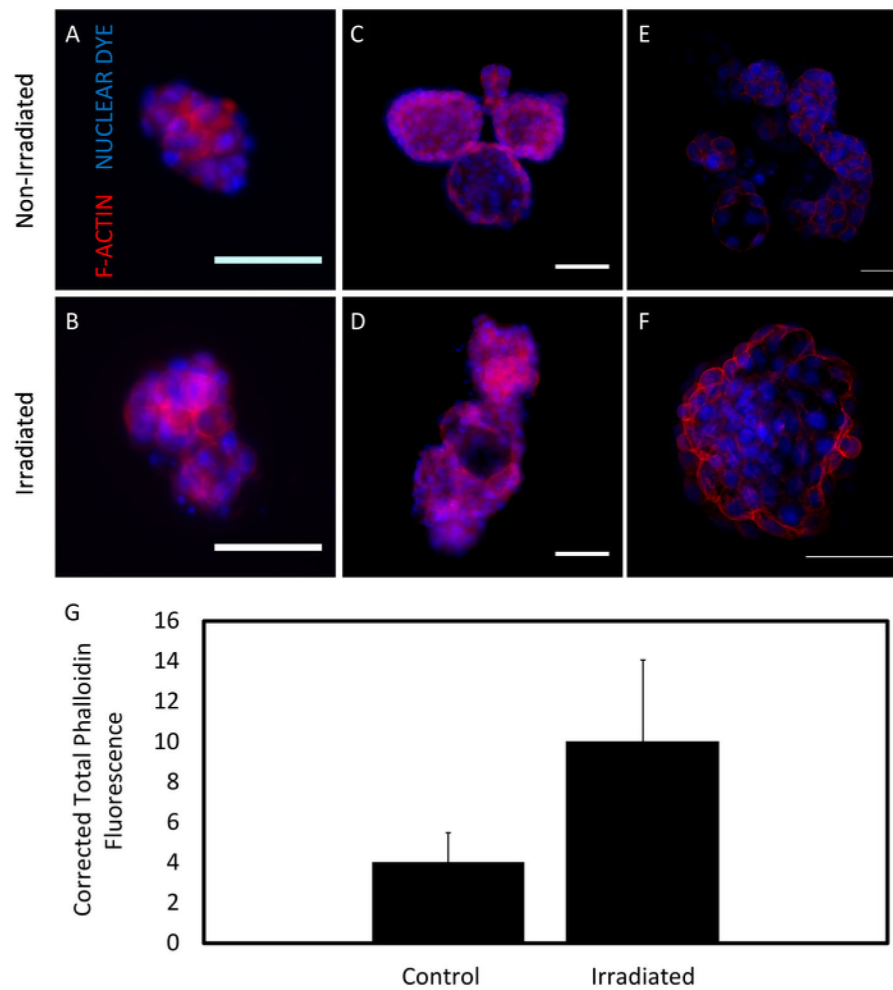


**Figure 5. F-actin expression in organoids.**

F-actin (red), a microfilament in epithelial cells, was expressed with lower intensity in non-irradiated organoids (**A, C, E**) than in irradiated (**B, D, F**) organoids. A nucleic acid stain was used to visualize nuclei (blue). Images were taken on low adhesion 96-well plates (**A, B**) and 16-well chamber slides (**C, D**). Images were also taken using confocal microscopy (**E, F**). All organoids were fixed and imaged after one week of growth. Scale bars are 50  $\mu\text{m}$ . **G**. Phalloidin fluorescence data from low adhesion plate images were quantified in ImageJ ( $n = 3$  glands). Error bars indicate standard error. Please click here to view a larger version of this figure.

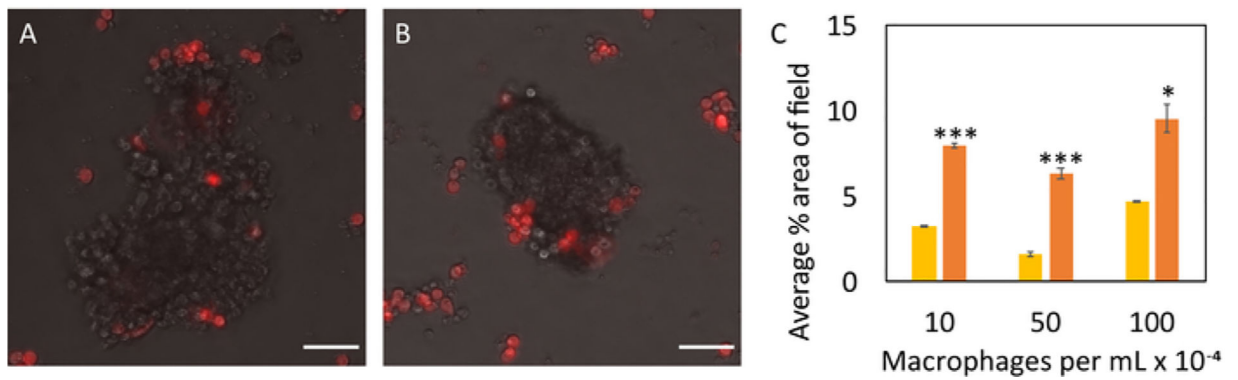


**Figure 6. Evaluating cell-cell interactions through macrophage-organoid co-culture.**

Macrophages (red) infiltrated control (A) and irradiated (B) organoids. Scale bars represent 50  $\mu\text{m}$ . Average percent area of macrophages in the image field (C) was reported at 24 hours of co-culture for control (yellow) and irradiated (orange) organoids ( $n=3$  glands for each sample). Macrophages were seeded at concentrations of 10,000 cells/mL, 50,000 cells/mL, and 100,000 cells/mL, and their infiltration was captured every 30 minutes via live cell fluorescence imaging. All co-culture experiments commenced 7 days after initial organoid seeding. Statistical significance was determined using a two-tailed, unpaired t-test, \* $p<0.05$ , \*\*\* $p<0.0001$ . Please click here to view a larger version of this figure.